Photoluminescence properties of *in situ* Tm-doped $Al_xGa_{1-x}N$

U. Hömmerich[a] and Ei Ei Nyein
Department of Physics, Hampton University, Hampton, Virginia 23668

D. S. Lee and A. J. Steckl
University of Cincinnati, Nanoelectronics Laboratory, Cincinnati, Ohio 45221

J. M. Zavada
US Army Research Office, Durham, North Carolina 27709

We report on the photoluminescence (PL) properties of *in situ* Tm-doped $Al_xGa_{1-x}N$ films ($0 \leqslant x \leqslant 1$) grown by solid-source molecular-beam epitaxy. It was found that the blue PL properties of $Al_xGa_{1-x}N$:Tm greatly change as a function of Al content. Under above-gap pumping, GaN:Tm exhibited a weak blue emission at ~478 nm from the $^1G_4 \rightarrow {}^3H_6$ transition of Tm^{3+}. Upon increasing Al content, an enhancement of the blue PL at 478 nm was observed. In addition, an intense blue PL line appeared at ~465 nm, which is assigned to the $^1D_2 \rightarrow {}^3F_4$ transition of Tm^{3+}. The overall blue PL intensity reached a maximum for $x=0.62$, with the 465 nm line dominating the visible PL spectrum. Under below-gap pumping, AlN:Tm also exhibited intense blue PL at 465 and 478 nm, as well as several other PL lines ranging from the ultraviolet to near-infrared. The Tm^{3+} PL from AlN:Tm was most likely excited through defect-related complexes in the AlN host. © 2003 American Institute of Physics. [DOI: 10.1063/1.1631742]

Light emission from rare-earth (RE)-doped III-N semiconductors is of significant current interest for applications in electroluminescence (EL) devices.[1-4] Previous work on visible emission from RE-doped III-Ns was mainly focused on RE-doped GaN.[1-3] Photoluminescence (PL) and cathodoluminescence (CL) data have been reported from nearly all lanthanide ions doped into GaN.[1-3] Visible EL devices based on RE-doped GaN, however, have only been demonstrated from GaN:Eu (red),[1,5,6] GaN:Er (green),[7] and GaN:Tm (blue).[8] One of the main challenges in using RE-doped GaN for full-color display applications is obtaining efficient blue emission. While dominant blue emission has been reported from GaN:Tm EL devices,[8,9] the overall device efficiency was significantly lower than results obtained for GaN:Eu (red) and GaN:Er (green).[2] For RE-doped AlN, red emission has also been reported from Eu, and green emission from Er- and Tb-doped amorphous and crystalline films.[10-12] Recently, blue CL was reported from Tm-impanted AlN[13] and efficient blue EL was demonstrated from *in situ* Tm-doped AlGaN films.[14]

In this letter, we report on the PL properties of $Al_xGa_{1-x}N$:Tm films under above- and below-gap pumping. Tm-doped $Al_xGa_{1-x}N$ films with $x=0$ (GaN), 0.16, 0.29, 0.39, 0.62, 0.81, and 1 (AlN) were grown by solid-source molecular-beam epitaxy on p-type Si (111) substrates. Elemental Al, Ga, and RE sources were used in conjunction with a rf-plasma source supplying atomic nitrogen. The Tm cell temperature was fixed at $600\,°C$, leading to a Tm concentration between ~0.2 and ~0.5 at. %. The $Al_xGa_{1-x}N$:Tm films were grown for 1 h at $550\,°C$ and a growth rate of ~0.5 μm/h. Adjusting the Al cell temperature during growth controlled the Al content in the films. The total flux of Ga and Al was kept constant. The PL was excited using the UV output (250 nm, 10 ns pulses, 10 Hz repetition rate) of an optical parametric oscillator (OPO) system. For low-temperature PL measurements, the samples were mounted on the cold finger of a closed-cycle helium refrigerator. Visible PL spectra were recorded using a 0.5 m monochromator equipped with a photomultiplier tube for light detection. The signal was processed using a boxcar averager, and PL lifetime transients were recorded using a digitizing oscilloscope.

Figure 1 shows an overview of the normalized PL spectra of Tm-doped $Al_xGa_{1-x}N$ with $x=0$, 0.16, 0.21, 0.39, 0.62, and 0.81. The calculated bandgap energies using Vegard's law and a bowing parameter of $b=1$ are 3.39 eV (GaN), 3.71, 3.82, 4.26, 4.91, and 5.56 eV, respectively.[15] The PL was excited using the 250 nm (~4.96 eV) output of an OPO system, which corresponds to above-gap pumping for $Al_xGa_{1-x}N$ samples with $x \leqslant 0.62$. Similar to previous reports,[8,9] the visible PL from GaN:Tm is characterized by a broad band extending from ~400 to 600 nm and near-band-edge emission at ~367 nm. A weak blue PL line located at ~478 nm from the $^1G_4 \rightarrow {}^3H_6$ transition of Tm^{3+} is hardly observable. The infrared PL at ~803 nm is tentatively assigned to the intra-$4f$ transition $^3H_4 \rightarrow {}^3H_6$ of Tm^{3+} ions.[9] Changing from GaN:Tm to $Al_xGa_{1-x}N$:Tm led to pronounced changes in the PL properties. Upon increasing Al content, the 478 nm PL line gained in intensity and was clearly observed. The broadband emission was also sharply reduced. The strongest emission from the $^1G_4 \rightarrow {}^3H_6$ transition at 478 nm was obtained for $x=0.39$. Interestingly, two other PL lines were observed: a weaker line at ~370 nm and a dominant blue line at ~465 nm. The PL intensity of the 465 nm line was several times larger compared to the 478 nm PL. The overall strongest blue PL intensity was measured
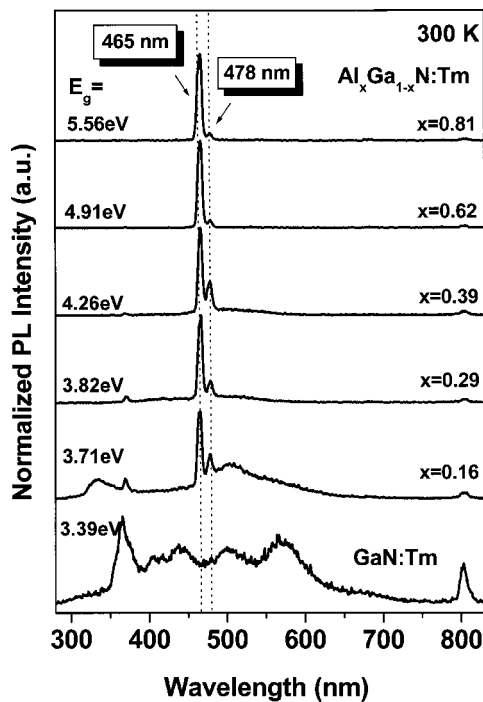
[a]Electronic mail: uwe.hommerich@hamptonu.edu

FIG. 1. Room-temperature PL spectra of $Al_xGa_{1-x}N$:Tm excited at 250 nm. The dotted lines indicate the position of the blue PL arising from the transitions $^1G_4 \rightarrow {}^3H_6$ (~478 nm) and $^1D_2 \rightarrow {}^3F_4$ (~465 nm). The calculated bandgap energies (E_g) are also indicated in the figure.
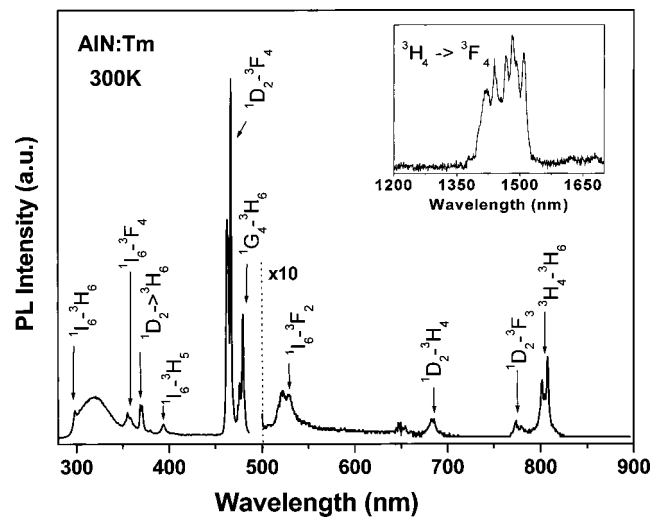

FIG. 2. High-resolution PL spectrum of AlN:Tm at room temperature. The PL was excited at 250 nm, which correspond to below-gap pumping. The assignment of the intra-$4f$ transitions of Tm^{3+} is indicated in the figure. The inset shows the infrared PL spectrum around 1450 nm.

from $Al_{0.62}Ga_{0.38}N$:Tm with the 465 nm line being roughly ten times more intense than the 478 nm line.

The observation of new PL lines in $Al_xGa_{1-x}N$:Tm can be explained by the change in bandgap energy of the host. Tm^{3+} has higher excited states above the $^1G_4$ level, which are located at ~3.4 eV ($^1D_2$) and ~4.2 eV ($^1I_6/{}^3P_0$).[16,17] The energy of the $^1D_2$ level is very similar to the bandgap energy of GaN (see Fig. 3). Therefore, no emission from the $^1D_2$ level is observed from GaN:Tm. Upon increasing the bandgap energy of $Al_xGa_{1-x}N$, the D_2 level moves within the bandgap of the host, which results in the observation of PL lines at 370 and 465 nm. Based on the comparison to existing literature,[16,17] the 370 and 465 nm lines are assigned to the $^1D_2 \rightarrow {}^3H_6$ and $^1D_2 \rightarrow {}^3F_4$ transitions of Tm^{3+}.

Figure 1 also indicates that the excitation efficiency of the $^1G_4$ level of Tm^{3+} is enhanced in $Al_xGa_{1-x}N$:Tm samples compared to GaN:Tm. As mentioned earlier, hardly any blue Tm^{3+} PL was observed in GaN:Tm. A similar poor above-gap pumping efficiency was reported for Tb^{3+} ions in GaN:Tb.[18] The weak PL excitation efficiency was explained using a defect-related energy transfer model as proposed by Takahei et al. for RE-doped semiconductors.[19] In this model, RE doping of a semiconductor leads to the formation of RE-related levels in the bandgap of the host. These levels can trap free carriers, which subsequently recombine and transfer their energy to intra-$4f$ RE transitions. Recent studies have identified RE-related traps for GaN:Eu,[19,20] GaN:Tb,[19] and GaN:Er[21] at ~0.3–0.4 eV below the conduction band of GaN. The recombination energy of carriers trapped at the RE-related defects in GaN is then estimated to be ~3.0–3.1 eV, which energetically matches intra-$4f$ transitions of Eu^{3+} and Er^{3+}, respectively.[16] On the other hand, Tb^{3+} ions do not exhibit intra-$4f$ transitions in that energy range, prevent-

ing an efficient carrier-mediated excitation process in GaN:Tb. Assuming that Tm^{3+} also induces a defect-level in GaN, similar arguments for the weak above-gap excitation efficiency can be applied to GaN:Tm Within the defect-related energy transfer model, however, the excitation efficiency of the Tm^{3+} can be optimized by a modification of the bandgap energy. Upon increasing Al content, higher excited states of Tm^{3+} ($^1D_2/{}^1I_6/{}^3P_J$) move within the bandgap of $Al_xGa_{1-x}N$, which provide additional channels for the energy transfer between defect levels and Tm^{3+} ions. Future investigations are necessary to identify Tm-related defects in $Al_xGa_{1-x}N$:Tm to support the defect-related energy transfer model. In addition, it cannot be excluded that chemical effects related to the presence of Al change the Tm^{3+} incorporation and excitation mechanisms, similar to observations made for Er-doped AlGaAs.[22]

The high-resolution PL spectrum, with excitation at 250 nm, of AlN:Tm at room temperature is shown in Fig. 2. The PL was dominated by intense blue PL lines centered at ~465 and ~478 nm. The average lifetimes of the 465 and 478 nm lines were determined to be ~2 and ~33 μs, respectively. The lifetimes were nearly temperature independent, suggesting that nonradiative decay processes are small. The different
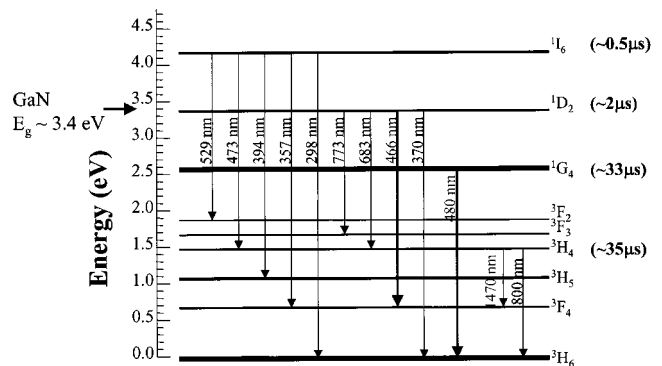

FIG. 3. Free-ion energy level diagram of Tm^{3+} ions and observed transitions in AlN:Tm. The bandgap of GaN is also indicated in the figure, along with PL lifetimes for several excited states of Tm^{3+}.
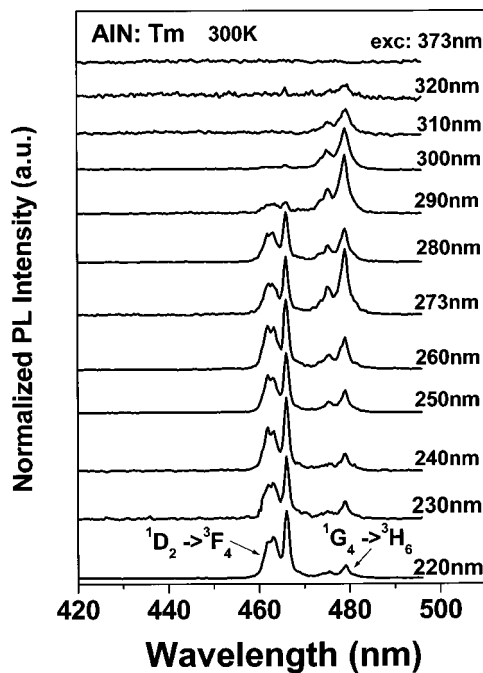
FIG. 4. Below-gap pumping of AlN:Tm using different excitation wavelengths in the UV region. The blue PL from Tm^{3+} can be excited of a wide range of wavelengths from ~320 down to 220 nm (lower wavelength limit of OPO laser system).

the $^1D_2$ (~465 nm) and $^1G_4$ (~478 nm) levels varied as a function of excitation wavelength. This result suggests the existence of different Tm^{3+} centers, which are selectively excited through different defects.

In summary, the PL properties of $Al_xGa_{1-x}N$:Tm were investigated. Under above-gap pumping, GaN:Tm exhibited only a weak blue emission from the $^1G_4 \rightarrow {}^3H_6$ transition of Tm^{3+}. A significant enhancement of the blue Tm^{3+} emission was observed from Tm-doped $Al_xGa_{1-x}N$ samples. Besides emission from the $^1G_4 \rightarrow {}^3H_6$ transition, a second blue emission line appeared around 465 nm, which was assigned to the $^1D_2 \rightarrow {}^3F_4$ transition of Tm^{3+}. The overall strongest blue PL emission was measured from $Al_xGa_{1-x}N$:Tm with $x = 0.62$. Strong blue emission from the $^1D_2$ and $^1G_4$ levels of Tm^{3+} was also observed from AlN:Tm under below-gap excitation. The large sensitivity of the blue emission from Tm^{3+} on the Al content of $Al_xGa_{1-x}N$ indicates the possibility to optimize the RE excitation and emission properties through careful bandgap engineering of the host.

lifetimes also provide further support that the two blue PL lines arise from different transitions of Tm^{3+}, namely, $^1D_2 \rightarrow {}^3F_4$ (465 nm) and $^1G_4 \rightarrow {}^3H_6$ (478 nm). Besides the dominant blue PL, AlN:Tm exhibited several weaker PL lines ranging from the UV to the near-infrared spectral region. Emission at 1440 nm was also observed from AlN:Tm (inset of Fig. 2), which arises from the well-known Tm^{3+} transition $^3H_4 \rightarrow {}^3F_4$.[17] The identification of the remaining PL lines was facilitated by a careful analysis of PL lifetimes. It was found that the Tm^{3+} PL originates from four excited states of Tm^{3+}, namely, the $^1I_6$, $^1D_2$, $^1G_4$, and $^3H_4$ with room-temperature lifetimes of ~0.5, ~2, ~33, and ~35 μs, respectively (Fig. 3). Since the $^1G_4$ and $^3H_4$ states have similar PL lifetimes, the origin of the ~805 nm PL was clarified by pumping resonantly into the $^1G_4$ and $^3F_2$ excited state at ~478 and ~675 nm, respectively. Moreover, since the ~805 nm PL can be pumped resonantly in the $^3F_2$ excited state, it has to be due to the $^3H_4 \rightarrow {}^3H_6$ transition of Tm^{3+}. Based on the comparison to Tm^{3+}-doped insulating materials,[16,17] we tentatively located the $^1I_6$ level below the $^3P_0$ state. A final identification of the energy position of $^1I_6$ and $^3P_0$ levels, however, requires further investigations.

It is also interesting to note that the Tm^{3+} PL was efficiently excited below the bandgap of AlN using the 250 nm output from an OPO system. Since Tm^{3+} has no intra-4f transition absorption line close to 250 nm,[16] the excitation of Tm^{3+} ions in AlN must occur through defects in the AlN host. A similar below-gap excitation mechanism was observed for AlN:Er.[23] Excitation-wavelength-dependent studies showed that the Tm^{3+} PL can be excited over a wide wavelength range starting from ~320 down to 220 nm, as shown in Fig. 4. It can be seen that the ratio of emission from

[1] A. J. Steckl and J. M. Zavada, Mater. Res. Bull. **24**, 33 (1999).
[2] A. J. Steckl, J. C. Heikenfeld, D. S. Lee, M. J. Garter, C. C. Baker, Y. Wang, and R. Jones, IEEE J. Sel. Top. Quantum Electron. **8**, 749 (2002).
[3] Mater. Res. Soc. Symp. Proc. **422** (1996).
[4] *Proceedings of E-MRS Symposium Spring 2000*, edited by J. Zavada, T. Gregorkiewicz, and A. J. Steckl [Mater. Sci. Eng., B **81**, (2001)].
[5] S. Morishima, T. Maruyama, M. Tanaka, Y. Masumoto, and K. Akimoto, Phys. Status Solidi A **76**, 113 (1999).
[6] J. Heikenfeld, M. Garter, D. S. Lee, R. Birkhahn, and A. J. Steckl, Appl. Phys. Lett. **75**, 1189 (1999).
[7] A. Steckl and R. Birkhahn, Appl. Phys. Lett. **73**, 1700 (1998).
[8] A. J. Steckl, M. Garter, D. S. Lee, J. Heikenfeld, and R. Birkhahn, Appl. Phys. Lett. **75**, 2184 (1999).
[9] D. S. Lee and A. J. Steckl, Appl. Phys. Lett. **82**, 55 (2003).
[10] W. M. Jadwisienczak, H. J. Lozykowski, I. Berish, A. Bensaoula, and I. G. Brown, J. Appl. Phys. **89**, 4384 (2001).
[11] K. Gurumurugan, H. Chen, G. R. Harp, W. M. Jadwisienczak, and H. J. Lozykowski, Appl. Phys. Lett. **74**, 3008 (1999).
[12] V. I. Dimitrova, P. G. Van Patten, H. H. Richardson, and M. E. Kordesh, Appl. Phys. Lett. **77**, 478 (2000).
[13] U. Vetter, M. F. Reid, H. Hofsaas, C. Ronning, J. Zenneck, M. Dietrich, and ISOLDE Collaboration, MRS Proceedings **743**, L6.16.1 (2003).
[14] D. S. Lee and A. J. Steckl, Appl. Phys. Lett. **83**, 2094 (2003).
[15] D. G. Ebling, L. Kirste, K. W. Benz, N. Teofilov, K. Thonke, and R. Sauer, J. Cryst. Growth **227–228**, 453 (2001).
[16] G. H. Dieke, *Spectra and Energy Levels of Rare Earth Ions in Crystals* (Wiley, New York, 1968).
[17] M. D. Seltzer, J. B. Gruber, M. E. Hills, G. J. Quarles, and C. A. Morrison, J. Appl. Phys. **74**, 2821 (1993).
[18] H. Bang, S. Morishima, Z. Li, K. Akimoto, M. Nomura, and E. Yagi, Phys. Status Solidi B **228**, 319 (2001).
[19] K. Takahei, A. Taguchi, H. Nakagome, K. Uwai, and P. S. Whitney, J. Appl. Phys. **66**, 4941 (1989).
[20] E. E. Nyein, U. Hommerich, J. Heikenfeld, D. S. Lee, A. J. Steckl, and J. M. Zavada, Appl. Phys. Lett. **82**, 1655 (2003).
[21] S. Kim, S. J. Rhee, X. Li, J. J. Coleman, S. G. Bishop, and P. B. Klein, J. Electron. Mater. **27**, 246 (1998).
[22] T. Zhang, J. Sun, N. V. Edwards, D. E. Moxey, R. M. Kolbas, and P. J. Caldwell, Mater. Res. Soc. Symp. Proc. **301**, 257 (1993).
[23] X. Wu, U. Hömmerich, J. D. Mackenzie, C. R. Abernathy, S. J. Pearton, R. N. Schwartz, R. G. Wilson, and J. M. Zavada, Appl. Phys. Lett. **70**, 2126 (1997).